COMPARISON OF CHANGE DETECTION METHODS FOR A RESIDUAL OF A HYDRAULIC SERVO-AXIS

Marco Muenchhof * **Rolf Isermann** *

* *Darmstadt University of Technology, Institute of Automatic Control, Landgraf-Georg-Strasse 4, 64283 Darmstadt, Germany,*
E-mail: {mmuenchhof,risermann}@iat.tu-darmstadt.de

Abstract: Different methods for change detection of signal features are compared for a residual generated at a hydraulic servo axis. The residual is based on a physical model of the pressure buildup inside the hydraulic cylinder. Nevertheless, it is augmented with an observer to counteract slight model impurities even over prolonged periods of operation. Different sensor faults are introduced, which affect the mean and/or the variance of the residual. Methods have been implemented, which allow to detect changes in the mean and variance of a signal. These methods are compared in terms of the size of the smallest detectable fault, time-to-detection and computational expense. All results have been verified experimentally. *Copyright© 2005 IFAC*

Keywords: hydraulic actuators, detection algorithms, alarm systems, fault detection

1. INTRODUCTION

Today, hydraulics are used in manifold areas of applications, ranging from shipbuilding and aeronautics to industrial machines and process automation. Many of these areas of applications are safety-critical (e. g. aeronautics) and thus have an ever-thriving demand for fault detection and fault diagnosis methods as to detect possibly severe faults early enough in order to initiate counter-measures or to reach a safe state before the faulty system comes into danger.

For a long time, fault detection in hydraulic systems was based on relatively simple methods such as monitoring the hydraulic fluid for debris or mounting expensive flow meters to monitor the hydraulic flow in and out of components (Watton, 1992).

With the advent of mechatronic systems (Isermann, 2003), i. e. the spatial and functional integration of electric, electronic, mechanic and information processing components, it is now possible to augment the system functionality with advanced fault detection and diagnosis methods, such as model-based fault detection and diagnosis (Isermann, 1997; Gertler, 1998; Isermann, 2005).

Two typical model-based fault detection methods are *parity equations* and *parameter estimation* (Höfling, 1996). For parity equations, a model of the process is run in parallel to the process and e. g. the deviation between the model output and the plant output is constantly monitored. In the fault free case, both outputs should match and thus the arithmetic difference between them should be close to zero. In the faulty case, the two outputs will depart from each other and thus their difference will deviate perceivably from zero. The models used can e. g. be analytical models or neural nets (Ramdén, 1998; Ramdén *et al.*, 1995). In this paper, the residuals will be generated using parity equations. Another approach is to extract parameters from the input-output behavior of the process, e. g. using an Extended Kalman Filter (Kress, 2002; Kazemi-Moghaddam, 1999).

The residual must then be monitored for changes. These *change detection methods* typically monitor characteristic statistical properties of the signal, such

as the mean and variance. There are different approches to monitor changes in the mean and variance of signals as e. g. reported in (Basseville and Nikiforov, 1993; Basseville, 2003; Moseler, 2001; Füssel, 2001). The paper at hand will examine these different methods and compare them with respect to the size of the smallest detectable fault, the time-to-detection and their computational expense. This comparison will be based on experimental data obtained at a hydraulic servo-axis.

The paper is divided as follows: In Section 2, the algorithms will be shortly introduced. This is then followed by a description of the testbed and the examined residual. Section 4 is concerned with the sensitivity of the proposed methods. It is examined which minimal fault size can be detected by the different methods. Next, the time-to-detection is discussed, which is another important quantity in the evaluation of fault detection methods. Finally, the computional expense is looked at in Section 6. This is another important aspect since all algorithms have to run in real-time. The reaction of the residual to a fault will be shown in Section 7. Conclusions (Section 8) end this paper.

2. INTRODUCTION TO THE ALGORITHMS

The simplest way to monitor changes in a signal x is to constantly compare the signal values against an upper and a lower threshold,

$$x < x_{upper}, \quad x > x_{lower}. \tag{1}$$

This is termed *limit checking* and is a computationally quite inexpensive technique. However, many signals, such as e. g. a residual, are noisy due to model impurities, process and sensor noise, etc. Therefore, the thresholds have to be increased to avoid false alarms. However, increasing the thresholds means that small changes in the signal might not be detected.

More advanced methods monitor statistically characteristic quantities of the signal, such as the *mean* and *variance*. The mean of a discrete time signal of length N is defined as (Papoulis, 1991)

$$\mu_x = \frac{1}{N}\sum_{i=1}^{N} x(i) \tag{2}$$

and the variance is given as

$$\sigma_x^2 = \frac{1}{N-1}\sum_{i=1}^{N} (x(i)-\mu_x)^2. \tag{3}$$

These calculations are only suitable for the offline calculation of time invariant statistical quantities. However, fault detection algorithms are typically implemented online and furthermore, the statistical quantities are time-varying. The fault will come into existence at some unspecified time instant t_F, thus the mean and variance will change around this time instant. This will lead to the recursive versions of Eq. 2 and Eq. 3,

$$\mu_x(k) = \mu_x(k-1) + \frac{1}{k}\left(x(k) - \mu_x(k-1)\right) \tag{4}$$

$$\sigma_x^2(k) = \frac{k-2}{k-1}\sigma_x^2(k-1) + \frac{1}{k}\left(x(k) - \mu_x(k-1)\right)^2 \tag{5}$$

Furthermore, the mean and variance can be calculated over a *time window* of finite length N, see e.g. (Moseler, 2001). At the discrete time k, these quantities can be calculated as

$$\mu_x(k) = \frac{1}{N}\sum_{i=k-N+1}^{k} x(i) \tag{6}$$

$$\sigma_x^2(k) = \frac{1}{N-1}\sum_{i=k-N+1}^{k} \left(x(i) - \mu_x(k)\right)^2. \tag{7}$$

Time-Window Average and Variance: The formulations in Eq. 6 and Eq. 7 are computationally expensive. An alternative is to apply recursive calculations. The mean can be calculated as

$$\mu_x(k) = \mu_x(k-1) + \frac{1}{N}\left(x(k) - x(k-N)\right) \tag{8}$$

and the recusive equation for the variance is given as

$$\begin{aligned}\sigma_x^2(k) = \sigma_x^2(k-1) + \frac{1}{N-1}\Big(&\left(x(k)-\mu_x(k)\right)^2 \\ &- \left(x(k-N)-\mu_x(k)\right)^2 + \frac{1}{N}\left(x(k)-x(k-N)\right)^2\Big)\end{aligned} \tag{9}$$

The performance of these two algorithms can be tuned by changing the window length N. Changes in the signal can now be monitored by comparing the estimates of the mean and variance against fixed thresholds.

There exists a couple of other well-known algorithms, which can detect changes in the mean and variance of a signal. A description of these methods can e. g. be found in (Basseville and Nikiforov, 1993). The key concepts generating *test quantities* will shortly be summarized in the following:

Shewart Control Chart: This test, as all following tests can discern between two hypotheses. These hypotheses state that the variable θ has the value θ_0 (Hypothesis 0) or θ_1 (Hypothesis 1). In the following, it is assumed, that the signal samples under scrutiny are Gaussian-distributed with mean value μ and variance σ^2.

The Shewart control chart is now implemented to test for a change in the mean from μ_0 to μ_1. The *decision function* is given as

$$S_1^N = \frac{\mu_1-\mu_0}{\sigma^2}\sum_{i=1}^{N}\left(x_i - \mu_0 - \frac{\mu_1-\mu_0}{2}\right) \tag{10}$$

This decision function is tested against a conveniently chosen threshold h. Hypothesis 1 is true, if

$$S_1^N > h. \tag{11}$$

Now, the assumption that the mean in the fault free case is $\mu_0 = 0$ will be utilized. This allows a few simplifications,

$$\tilde{S}_1^N = \sum_{i=1}^{N} x_i \tag{12}$$

which is tested against a new threshold $\tilde{h}$.

Geometric Moving Average Control Chart: This method is based on the idea of using higher weights on recent observations and lower weights on past observations, which is also known under the term *exponential forgetting*. For a change in the mean of a Gaussian sequence, the decision function is given as

$$g(k) = (1-\alpha)g(k-1) + \alpha\,(x(k) - \mu_0)\,. \tag{13}$$

Once again, for $\mu_0 = 0$, the equation can be rewritten as

$$g(k) = (1-\alpha)g(k-1) + \alpha x(k). \tag{14}$$

The starting value can conveniently be chosen as $g(0) = 0$.

For a change in the variance from σ_0^2 to σ_1^2, the decision function is given as

$$g(k) = (1-\alpha)g(k-1) + \alpha\,(x(k) - \mu)^2\,. \tag{15}$$

Since the mean μ once again is zero, this equation can be rewritten as

$$g(k) = (1-\alpha)g(k-1) + \alpha\, x(k)^2. \tag{16}$$

with the starting value $g(0) = 0$.

Finite Moving Average Control Charts: Now, a finite memory is utilized with arbitrarely chosen weights. For a change in the mean, the decision function reads

$$g(k) = \sum_{i=0}^{N-1} \gamma_i\,(x_{k-i} - \mu_0) \tag{17}$$

The major disadvantage of this algorithm is the large number of parameters, since all γ_i must be tuned to achieve optimal performance of the algorithm. Since all other algorithms are much easier to tune and depend on one parameter only, this Finite Moving Average Control Chart will be left out of the comparison.

Cumulative Sum (CUSUM): For an increase in the mean, the algorithm is given as

$$g(k) = \left[g(k-1) + \frac{\mu_1 - \mu_0}{\sigma^2}\left(x(k) - \frac{\mu_1 + \mu_0}{2}\right)\right]^+, \tag{18}$$

where the function $y = [x]^+$ is defined as

$$y = \begin{cases} x \text{ if } x > 0 \\ 0 \text{ otherwise} \end{cases} \tag{19}$$

A decrease in the mean can be detected by a straightforward extension of Eq. 18.

Low Pass Filtering: Approximate estimations of the mean and variance can also be calculated by low pass filtering, see (Höfling, 1996). The corresponding block diagram is shown in Fig. 1. All the described methods will now be compared.

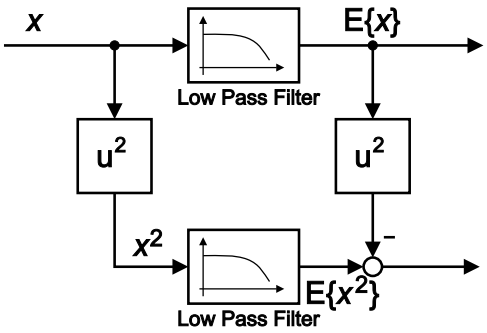

Fig. 1. Calculation of Mean and Variance by Low Pass Filtering

3. DESCRIPTION OF THE RESIDUAL OF A PARITY EQUATION

At a testbed consisting of a linear hydraulic servo-axis, the parity equation described in the following has been implemented. In the evaluation, the parity equation governing the hydraulics of the cylinder will be examined. The behavior of the system is highly nonlinear. The pressure buildup in chamber A of the hydraulic cylinder amounts to

$$\dot{p}_A = \frac{E(p_A)\,(\dot{V}_A - A_A\,\dot{x} - G_{AB}(p_A - p_B))}{V_{0A} + A_A\,x} \tag{20}$$

Here, E is the pressure dependent bulk modulus. A_A is the cross-sectional area and V_{0A} the volume at $x = 0$. G_{AB} is the coefficient of laminar leakage flow between chamber A and B. This flow depends on the pressure difference between chamber A, p_A, and B, p_B. All measured variables are also depicted in Fig. 2, which displays the schematic cross-sectional drawing of a proportional valve and cylinder as used at the hydraulic servo-axis.

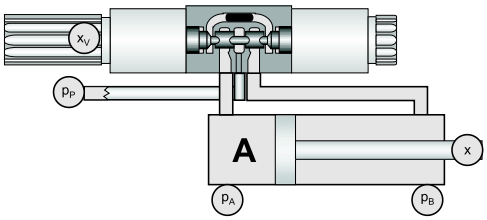

Fig. 2. Schematic View of a Hydraulic Servo-Axis

The displacement of the valve spool and the thereby determined opening of the control edges determines the flow into chamber A, $\dot{V}_A$, given by

$$\begin{aligned} \dot{V}_A = {} & B_{V1}(x_V)\sqrt{|p_P - p_A|}\,\mathrm{sign}\,(p_P - p_A) \\ & - B_{V2}(x_V)\sqrt{|p_A - p_T|}\,\mathrm{sign}\,(p_A - p_T)\,, \end{aligned} \tag{21}$$

where B_{V1} and B_{V2} are the spool displacement x_V dependent coefficients of turbulent flow across the control edges. p_P is the pressure at the pump and p_T is the pressure in the return line, whose influence is typically neglected ($p_T = 0$).

For the observer, Eq. 20 will be solved for $\dot{x}$ instead of $\dot{p}_A$

$$\dot{x} = \frac{1}{A}\left(\dot{V}_A - G_{AB}(p_A - p_B) - \dot{p}_A \frac{V_{0A} + A_A x}{E}\right) \quad (22)$$

In the literature, it is normally reported that Eq. 20 is implemented. However, the model governed by Eq. 22 is proposed as a basis for parity equations and observers, since the dynamics in $\dot{x}$ are much slower than those in $\dot{p}_A$. The high fidelity of this model allows to run the model in parallel to the plant without the need for an observer-based feedback scheme for the output error over a short time period. Figure 3 shows the open loop-response of the model to an APRBS input. An equation similar to Eq. 22 can

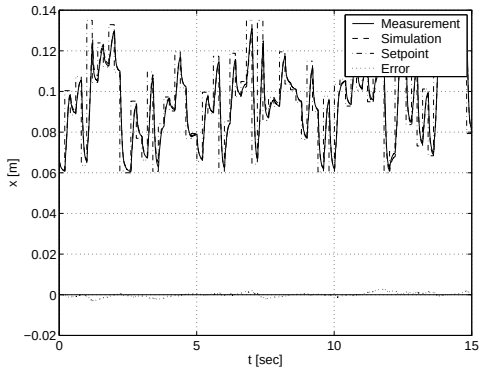

Fig. 3. Comparison of Open Loop Model and System Response

be implemented for chamber B of the differential cylinder.

To avoid that the model output departs from the system output over extended time periods, an observer will now be introduced into the system. The output error is fed back amplified by an observer gain h. The observer block diagram is shown in Fig. 4. The output error,

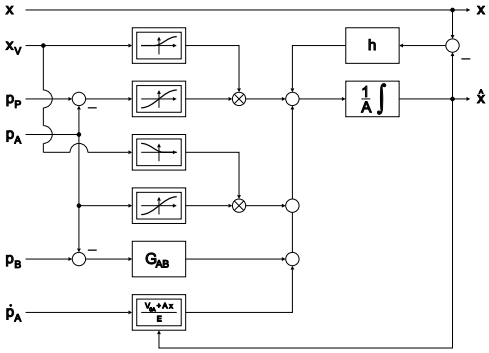

Fig. 4. Block Diagramm of the Observer for Correcting the Model Output, $\hat{x}(t)$ of the servo-axis

$$r = \hat{x} - x, \quad (23)$$

will now be used as a residual. In the fault free case, the residual should have zero mean. In the presence of the faults, the observer has to constantly adapt the model output to the process output and thus the variance and/or the mean of the residual will change.

4. SMALLEST DETECTABLE FAULT

The following methods have been compared:

(1) Limit checking, Eq. 1
(2) Time-window average with parameter window length N, Eq. 8
(3) CUSUM test for increase in mean with parameter threshold $\tilde{h}$, Eq. 18
(4) CUSUM test for decrease in mean with parameter threshold $\tilde{h}$, analog to Eq. 18
(5) Shewart Control Chart with parameter window length N, Eq. 12
(6) GMA for mean with parameter forgetting factor α, Eq. 14
(7) GMA for variance with parameter forgetting factor α, Eq.16
(8) Estimation of mean with one low-pass filter of first order with parameter time constant T, Fig. 1
(9) Estimation of variance with two low-pass filters of first order with parameter time constant T, Fig. 1
(10) Estimation of mean with one low-pass filter of second order with parameter time constant T, Fig. 1
(11) Estimation of variance with two low-pass filters of second order with parameter time constant T, Fig. 1

All methods have at most one parameter. Offset faults for all sensors have been investigated. For the displacement sensor x, an offset fault will only lead to a temporary deflection of the residual, because of the feed-back structure. Therefore, this fault has not been considered in the comparison. Faults in sensor p_B do barely affect the residual and can much more easily be detected by reformulating Eq. 22 for chamber B. Therefore, this fault has also been neglected for a comparison. The other three faults have been numbered as follows:

(1) Fault in p_P
(2) Fault in p_A
(3) Fault in x_V

Table 1 shows the sensititvity to the individual faults. The bold number denotes the overall smallest detectable fault. The different methods have been tested with ten data sets recorded at the testbed. First, the reaction of the different methods to the fault free signals has been determined. Then, the thresholds for raising an alarm have been determined by adding a safety margin of 10%. In Fig. 5, the minimum detectable fault as a function of the tunebale parameter has been plotted. This diagramm illustrates that for all methods in fact the minimum has been found.

5. TIME-TO-DETECTION

Next, the time-to-detection is considered. This is another important quantity, since faults should be de-

Table 1. Smallest Detectable Fault of the Different Methods

Method	Fault 1	Fault 2	Fault 3
1	1.64 %	1.68 %	0.52 %
2	1.03 %	0.91 %	0.33 %
3	1.02 %	—	0.31 %
4	—	0.89 %	—
5	**0.89 %**	**0.78 %**	**0.28 %**
6	1.06 %	0.82 %	0.34 %
7	1.59 %	0.90 %	0.48 %
8	1.06 %	0.82 %	0.34 %
9	1.72 %	1.03 %	0.50 %
10	1.07 %	0.89 %	0.36 %
11	1.80 %	1.06 %	0.60 %

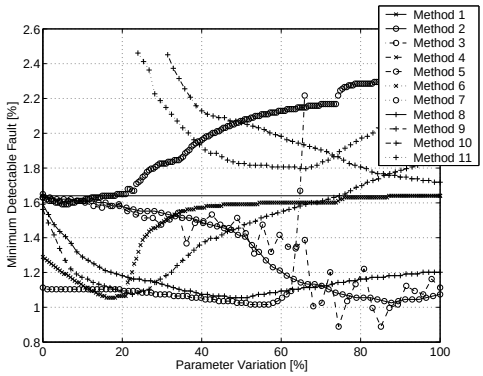

Fig. 5. Minimum Detectable Faultsize as a Function of Parameter Variation of the Tuneable Parameter for Sensor Fault p_P

tected near to their time-origin. The minimum detectable fault as a function of the final time is shown in Fig. 6. One can clearly see the trade-off between fault size and time-to-detection. It is difficult to compare the individual methods by the time to detect a certain fault size, since the individual methods differ quite much in their performance and their ability to detect a certain fault size.

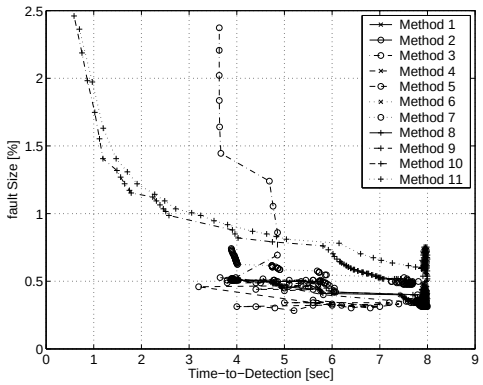

Fig. 6. Minimum Detectable Faultsize as a Function of Time-to-Detection for Sensor Fault 3

6. COMPUTATIONAL EXPENSE

Another important aspect is the computational expense, since in on-line fault detection applications, these algorithms must run in real-time. In Tab. 2, the

Table 2. Computational expense

Method	Sum of Operations
1	1
2	5
3	4
4	4
5	3
6	4
7	5
8	4
9	10
10	11
11	24

computational expense for the different algorithms is listed. In determining the computational expense, it has been assumed that the residual has zero mean. Otherwise, one subtraction has to be added to each algorithm for subtracting the (non-zero) mean from the actual value and thereby generating a zero mean sequence. Since multiplications are typically less expensive than divisions, all division with a constant divisor have been counted as multiplications. All tests have been implemented as one-sided tests.

7. RESIDUAL REACTION

In this section, the high sensitivity of the residual to faults will be shown. In Fig. 7, a 2% sensor offset for sensor x_V has been inserted after time $t = 4$ sec. One can see from the upper subplot that this small change is barely visible in the signal from the sensor. In the lower subplot, a time-window average with a window length of 1500 samples is shown. One can see the clear reaction to the inserted sensor fault. The time-of-origin of the fault is marked by the thick vertical line at $t = 4$sec. The upper and lower threshold are denoted by thick horizontal lines.

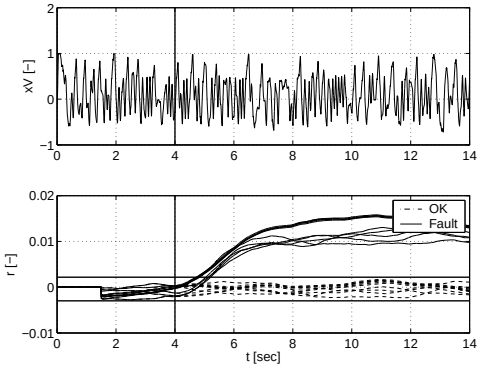

Fig. 7. Response of the Residual to a Sensor Offset in x_V

8. CONCLUSIONS

The individual algorithms will now be rated. This is shown in Tab. 3. The table evaluates the sensitivity (sens), time-to-detection (t-to-d) and the computational expense (comp exp).

Table 3. Rating of the Methods (+ + best, - - worst)

Method	Sens.	T-to-D	Comp. Exp.
1	- -	0	+ +
2	+	0	0
3	+	0	+
4	+	0	+
5	+ +	+ +	+
6	+	0	0
7	-	0	0
8	+	0	0
9	- -	+	-
10	+	- -	- -
11	- -	+	- -

Based on this table, method 5 performs best, which is the Shewart Control Chart. Methods 3 and 4 perform well both in the sensitivity as well as the computational expense. These methods represent the CUSUM algorithm. Method 2, 6, and 8 perform well with respect to the sensitivity. These are the Moving Average and the GMA for mean, as well as the estimation of mean with a low-pass filter of first order. SLightly worse performance is shown by the low-pass of second order and the low-pass filter estimation of the variance. This illustrates that the sensor faults considered change mainly the mean of the residuum and not so much the variance.

In Summary, it should first be mentioned that a new parity equation was proposed for the supervision of a linear-hydraulic servo axis. The high fidelity of the model allows to detect sensor faults as small as 2% or less reliably.

Then different methods have been compared which allow to detect changes in a residuum. These changes can stem from sensor and/or process faults. A total of eleven different methods has shortly been introduced and then compared with respect to the sensititviy, time-to-detection and the computational expense. Although the Shewart Control Chart algorithm performed best, there exist a couple of well-performing methods to detect changes in the mean and/or variance of a signal.

9. ACKNOWLEDGEMENT

This research work has been supported under grant AiF 12564 from budgetary resources of the *Bundesministerium für Wirtschaft und Technologie (BMWi)* by the *Arbeitsgemeinschaft industrieller Forschungsvereinigungen "Otto von Guericke" e. V. (AiF)*. The closing report is available from the *Deutsche Forschungsgesellschaft zur Anwendung der Mikroelektronik DFAM e. V.*. Furthermore, this research work was supported by *Bosch Rexroth AG, Lohr*.

REFERENCES

Basseville, Michèle (2003). Model-based statistical signal processing and decision theoretic approaches to monitoring. In: *Proceedings of the Safeprocess 2003*. Washington, DC (USA).

Basseville, Michèle and Igor V. Nikiforov (1993). *Detection of Abrupt Changes: Theory and Application*. Prentice Hall. Englewood Cliffs, NJ.

Füssel, Dominik (2001). *Fault Diagnosis with Tree-Structured Neuro-Fuzzy Systems, Nummer 957 in Fortschritt-Berichte VDI Reihe 8*. VDI-Verlag. Düsseldorf.

Gertler, J. (1998). *Fault Detection and Diagnosis in Engineering Systems*. Marcel Dekker. New York.

Höfling, T. (1996). *Methoden zur Fehlererkennung mit Parameterschätzung und Paritätsgleichungen, Nummer 546 in Fortschritt-Berichte VDI Reihe 8*. VDI-Verlag. Düsseldorf.

Isermann, Rolf (1997). Supervision, fault-detection and fault-diagnosis methods. *Control Engineering Practice* **5**(5), 639 – 652.

Isermann, Rolf (2003). *Mechatronic Systems : Fundamentals*. Springer Verlag. UK.

Isermann, Rolf (2005). *Fault Diagnosis and Fault Tolerance*. Springer Verlag. Berlin.

Kazemi-Moghaddam, Abbas (1999). Fehlerfrühidentifikation und -diagnose eines elektrohydraulischen Linearantriebssystems. PhD thesis. TU Darmstadt, Fachbereich Maschinenbau. Darmstadt. URL: http://elib.tu-darmstadt.de/diss/000025.

Kress, Richard (2002). Robuste Fehlerdiagnoseverfahren zur Wartung und Serienabnahme elektrohydraulischer Aktuatoren. PhD thesis. TU Darmstadt, Fachbereich Maschinenbau. Darmstadt. URL: http://elib.tu-darmstadt.de/diss/000336/.

Moseler, Olaf (2001). *Mikrocontrollerbasierte Fehlererkennung für mechatronische Komponenten am Beispiel eines elektromechanischen Stellanrtiebs, Nummer 908 in Fortschritt-Berichte VDI Reihe 8*. VDI-Verlag. Düsseldorf.

Papoulis, Athanasios (1991). *Probability, Random Variables and Stochastic Processes*. WCB McGraw-Hill. Boston.

Ramdén, Teresia (1998). Condition Monitoring and Fault Diagnosis of Fluid Power Systems : Dissertation No 514. PhD thesis. Linköping University, Sweden. Linköping.

Ramdén, Teresia, Petter Krus and Jan-Ove Palmberg (1995). Fault diagnosis of a complex fluid power system using neural networks. In: *Proceedings of the Fourth Scandinavian International Conference on Fluid Power*. Tampere (Finland).

Watton, John (1992). *Condition Monitoring and Fault Diagnosis in Fluid Power Systems*. Ellis Horwood. New York.